

Tribological Behavior of Thermally Sprayed Coatings with Different Chemical Composition and Modified by Remelting

E. Zdravecká^{a,*}, M. Ondáčá, J. Tkáčová^a

^aTechnical University of Košice, Faculty of Mechanical Engineering, Letná 9, 040 01 Košice, Slovakia.

Keywords:

Thermally flame sprayed coatings
Remelting
Chemical composition
Tribological behavior

ABSTRACT

Thermal spraying is a coating process combining various techniques to protect the materials from a variety of adverse tribological, mechanical, and thermal conditions. Ni-base alloys are widely used to obtain high wear/corrosion-resistant coatings. In the present study, the wear behavior of NiCrBSi self-fluxing alloy coatings deposited from the two innovative powders with efficient chemical compositions by the two-step deposition process was investigated under the three-body abrasion test. After wear tests, wear resistance was investigated, and the worn surfaces were characterized by SEM to determine the main mechanism. These innovative metallic powders with efficient chemical compositions show good wear performance for application in industry.

* Corresponding author:

Eva Zdravecká 
E-mail: eva.zdravecka@tuke.sk

Received: 29 July 2019

Revised: 27 September 2019

Accepted: 23 October 2019

© 2019 Published by Faculty of Engineering

1. INTRODUCTION

Thermal spraying offers techniques to protect the materials from a variety of adverse tribological, mechanical, and thermal conditions and provides a wide range of coatings with very different compositions and properties. Thermal spraying technology provides cost-effective processes in many industries for the application of wear and corrosion-resistant coatings and can be applied to a variety of materials [1-2].

Nickel-based alloys are widely used in spraying materials as they exhibit good resistance to wear, oxidation, and corrosion at high temperatures and are also low in cost [3-5]. Ni-based self-fluxing alloy coatings are the most

often deposited by high-velocity oxygen/air-fuel spraying (HVOF, HVOF), flame (gas) low-velocity spraying (LVOF), plasma spraying, laser cladding, and plasma transferred arc welding (PTA or PTAW). The problems with porosity and adhesion to the substrate influence the quality of the thermally sprayed coatings and their performance. It can be improved by subjecting coatings to remelting using various technologies (e.g., oxy-acetylene flame, furnace, electric resistance, and laser) [6-8]. Comparing to other techniques, the method of flame spraying with remelting is frequently used, versatile, and also economical [9,10].

The chemical composition and physical properties of coatings have a direct impact on

their performance [11]. Higher chromium content helps increase the resistance to oxidation and high-temperature corrosion and increases the hardness of the coating by the formation of hard precipitates. Boron lowers the melting point and promotes the formation of hard phases. Silicon is added to increase self-fluxing properties. Carbon produces carbides with high hardness levels that improve the wear resistance of coatings [12, 13]. The addition of phosphorus results in a lowering of the melting point, deoxidation of the nickel, and intensive reaction with the nickel [14]. Tungsten carbide (WC) and chromium carbide Cr_3C_2 [15] are the most commonly recommended phase reinforcement. Also, other materials are used as reinforcement phases such as TiC, SiC, WC-Co, Cr_3C_2 , and NBC, because of their high hardness and good wear resistance [16,17].

Most material properties (e.g., elastic modulus, yield strength, hardness or fracture toughness) well defined for metallic materials, do not have simple equivalents for thermally sprayed coatings. It is due to the complexity of thermally sprayed materials containing different phases and microstructures. Therefore, laboratory tests are commonly used as a quantitative tool to describe the wear behavior of the material tested. The abrasive wear is influenced by a number of different factors, such as the properties of the materials, the service conditions (applied load and abrasive grit size), and the environment (temperature and humidity). For evaluation of abrasive wear resistance, the three-body abrasion test is often used.

In the field of surface engineering, systematic research of materials is ongoing to identify correlations between the chemical composition of materials and tribological behavior. Research in this field was performed using NiCrBSi powder coatings high in Cr (14.5 %) and Fe (4.5 %) [18]. Another research has been carried out in this field using powder but with a higher Cr content (16.5 %) [19]. Similarly, other scientific works were carried out using a Ni-based alloy powder with a nominal chemical composition of Cr 14.8 %, B 3.1 %, Si 4.3 %, Fe 3.7 %, C 0.75 %, and Ni (tagged as Borotec 1000).

In the present study, the wear behavior of NiCrBSi self-fluxing alloy coatings deposited from the two innovative powders with efficient

chemical compositions (made by Welding Research Institute, PI, Slovakia, [14] by two-step deposition process on carbon steel was investigated under the three-body abrasion test according to the ASTM standard G65-4 known as the Dry-Sand Rubber Wheel (DSRW). After wear tests, wear resistance was investigated, and the worn surfaces were characterized by SEM to determine the main mechanism responsible for wear behavior.

2. EXPERIMENTAL PROCEDURE

Ni-based NiCrBSi alloys with different chemical compositions were used for flame spraying and remelting.

2.1 Materials

New designed metallic Ni-based self-fluxing alloy powders with an average granularity of $-100 \mu\text{m} + 45 \mu\text{m}$ and the melting point of 1010°C were applied as the coating material (Welding Research Institute, PI, Slovakia). The chemical composition of the spray powders (referred to as powders A and B) is shown in Table 1. Powders A and B were used to deposit the coatings by low-cost flame spraying method with remelting for abrasive wear applications.

Table 1. Chemical composition of powders

Powder	Chemical composition [%]						
	C	Si	Mn	P	Cr	Mo	B
A	0.25	3.9	0.08	0.001	0.12	0.01	0.98
	S:0.006, Fe:0.51, W:0.02, Cu:0.1, Co:0.02, Ti:0.02, Nb<0.0, Ni:94.49						
B	0.21	3.52	0.07	0.057	8.85	1.30	1.48
	S:0.012, Fe:2.63, V:0.01, W:0.02, Cu:0.73, Al:0.004, Co:0.02, Ti:0.01, Ni:81.4						

The powders morphology shows the spherical particles typically produced by the gas atomization process (Figs. 1 and 2). Spheroidal particles of powder B contain hard chromium carbides in the Ni matrix.

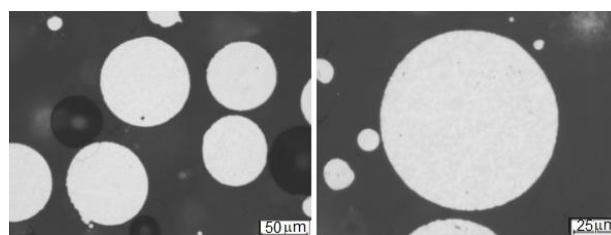


Fig. 1. The microstructure of powder B.

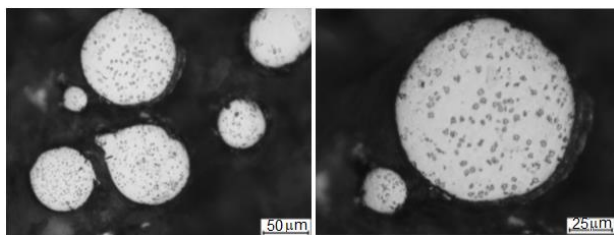


Fig. 2. The microstructure of powder B.

2.2 Coatings deposition

Coatings were sprayed on the plate (dimensions 100x150x8 [mm]) made of hot rolled low carbon steel S35530 EN10027-1 (1.0553) as substrate material by two-step flame-powder deposition technology prepared in Welding Research Institute, PI, Slovakia.

The surfaces of the blocks were shot-blasted (corundum) to eliminate grease and oxides and to stimulate the adhesion of the sprayed layers. The surface roughness before deposition processes was approximately $Ra \approx 5.0 \mu\text{m}$ to provide adhesion and to improve the contact properties. The coated samples for abrasion tests were cut by wire electro-discharge machining process from plate to dimensions of 75x22x7 [mm]. The surface of samples was ground to a roughness $Ra = 0.2 \mu\text{m}$ before the ASTM test. The number of samples for each experimental test was three. Before spraying, the samples were preheated to temperature from 90 °C to 100 °C to achieve good adhesion [2,20]. For the conventional thermal spray process, as established in technical literature, e.g. [21,22], an appropriate substrate temperature can enhance the adhesion of coatings.

The flame spraying process was carried out by the SuperJet Eutalloy thermal spraying gun. The applied pressures of gases were 100 kPa for oxygen and 70 kPa for acetylene. The spray distance between the gun and the substrate was approximately 200 mm because excessive stand-off distance produces a more porous and oxidized coating with reduced cohesion and adhesion. The sprayed coatings were submitted to a post thermal treatment (oxy-acetylene flame remelting) at a temperature of 1025 °C for the provision of diffusion processes. The thermally sprayed coatings obtained by this process show an improvement of bond strength between coating and substrate [5]. Figures 5 and 6 and a detailed SEM inspection (Figs. 9 and 10) confirm good adhesion.

2.3 Microstructure, hardness and wear test

Total coatings thickness was approximately 2.5 – 3 mm, as documented in Figs. 5 and 6. Microstructural investigations were carried out on a cross-section of samples using optical microscope Neophot 21 and SEM. Coatings were etched with a mixture of HF (10 cc) and HNO₃ (100 cc). The surface hardness HR15N was measured on the sprayed coatings surfaces after grinding using hardness tester Rockwell RB-1E/AQ. The reported values are average of at least 5 measurements. The coating micro-hardness HV0.3 was measured on the coatings cross-sections (Hanemann's hardness tester HV0.3). The reported values are an average of at least 10 measurements.

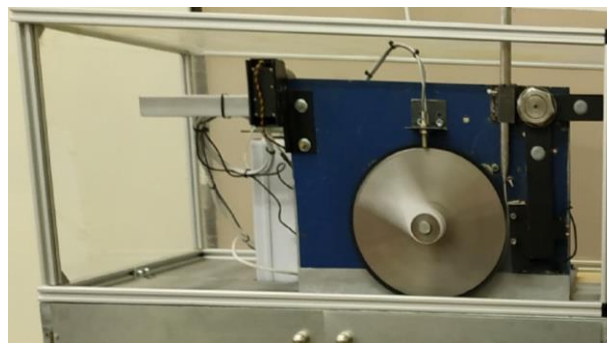


Fig. 3. Abrasion tester [23].

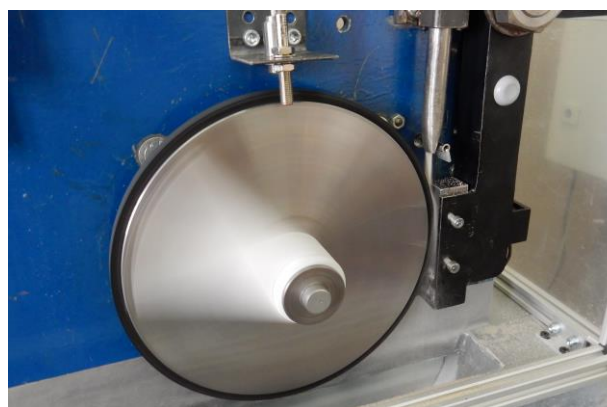


Fig. 4. The view on tribo-pair [23].

The investigations of the wear behavior were carried out under the abrasion regime. The test parameters of the three-body abrasion test were set according to the ASTM standard G65-4 known as the Dry-Sand Rubber Wheel (DSRW) test [23-25]. In this test, a stream of particles is fed through the loaded contact between a test specimen and a rotating rubber steel wheel; the abrasive particles pass through the contact region only once (Figs. 3 and 4). The constant test parameters were as follows: wheel speed of 2.3

m.s⁻¹, load 35 N, SiO₂ angular abrasive particle size of 0.2-0.315 mm with the hardness of 1000-1200 HV, and abrasion linear length of 1031 m, wheel diameter – 229 mm. Before the tests, the samples were ground to remove the oxide layer and to obtain the roughness according to ASTM G65 standard test. Before weighing, all samples were ultrasonically cleaned in distilled water. Weight loss was measured using an analytical balance KERN ABJ 320-4NM (measurement sensitivity: 0.1 mg) Samples were weighed before and after the test, recording the weight loss. The abrasion test was repeated three times for the materials used, and the average weight loss was calculated.

Weight loss was used as a measure of wear. The specific wear rate W_s [mm³/N.m] is usually expressed and calculated as follows:

$$W_s = \Delta V / (F_n \cdot L) \quad (1)$$

where: ΔV refers to wear volume [mm³],

F_n is normal load [N] per sliding distance L [m].

The volume loss ΔV [mm³] was calculated as follows:

$$\Delta V = \Delta m / \zeta \quad (2)$$

where: Δm is mass loss [g], ζ is density [g/mm³]. The weight loss obtained was converted to volume loss using the 7.082 g/mm³ value of coatings density.

SEM analysis of the worn surfaces was carried out for all coatings after tribotests. These investigations of the wear appearance can give important indications about the predominant wear mechanisms.

The roughness on worn surfaces of coatings was measured by surftester Mitutoyo SJ-301, according to DIN EN ISO 4287 (5 mm sampling length and 0.8 mm cut-off length). The reported values are the average of at least five measurements.

3. RESULTS AND DISCUSSION

The cross-section of the of coatings is shown in Figs. 5 and 6. The remelted coatings documented in Figs. 5 to 10 show low porosity. This is also consistent with the literature [26, 27] where it is indicated that complete densification cannot be obtained, but that porosity can be greatly reduced.

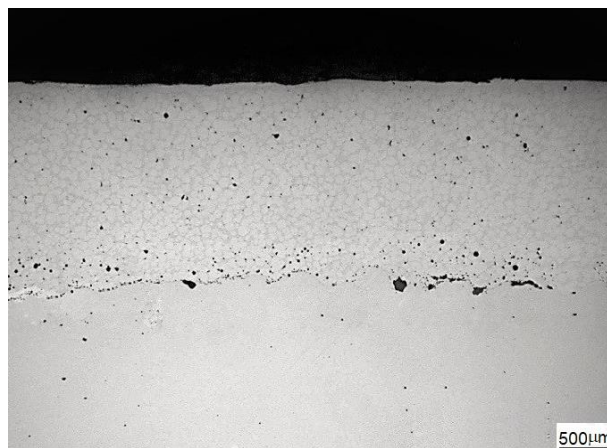


Fig. 5. The cross-section of coating A.

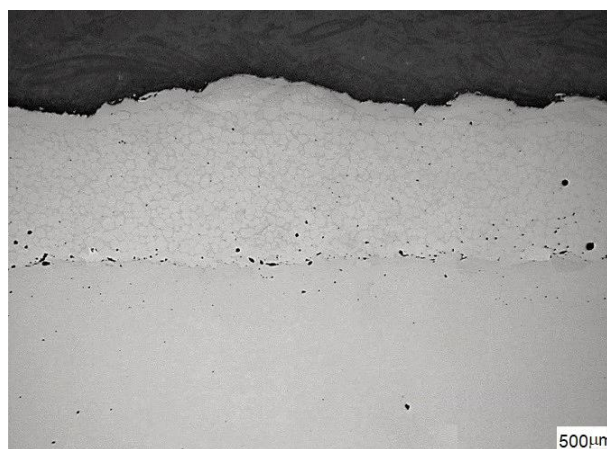


Fig. 6. The cross-section of coating B.

The Ni-based matrix contains nickel, chromium, iron, silicon, and boron. Binary phase diagrams such as NiCr, NiB, and NiSi provide information on the effects of individual alloying elements [28]. They show that the presence of Cr, Si, and B elements reduces the melting temperature point of nickel. Furthermore, these three elements play a role in forming hard borides and carbides, owing to improve the mechanical properties of the produced coating. The NiCrBSi is made of a Ni-rich solid solution phase 5-Ni and low content of Ni-Ni₃B eutectic [29]. When the spraying alloy solidified from high temperature, several possible borides, carbides, and silicates may be created, such as Ni₂B, CrB, Ni₅Si₃, Ni₁₃Si₁₂, Ni₃Si, (Cr,Fe)₇C₃ and Cr₂₃C₆ [30]. In accordance with the above mentioned, nickel compounds were observed in both coatings, the nickel solid solution (bright areas) is visible in Figs. 7 and 8. The grain size and shape of Ni cells of both coatings are different with the distribution of precipitates at the grain boundary. Figure 7 shows less numerous darker areas indicating fewer precipitates (hard phases), resulting in the

lower hardness of coating A. The precipitates (dark areas) in Fig. 8 have a polygonal shape with homogenous distribution in the Ni matrix.

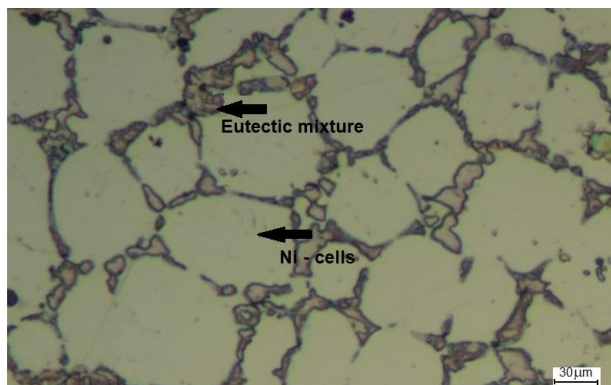


Fig. 7. The microstructure of coating A.

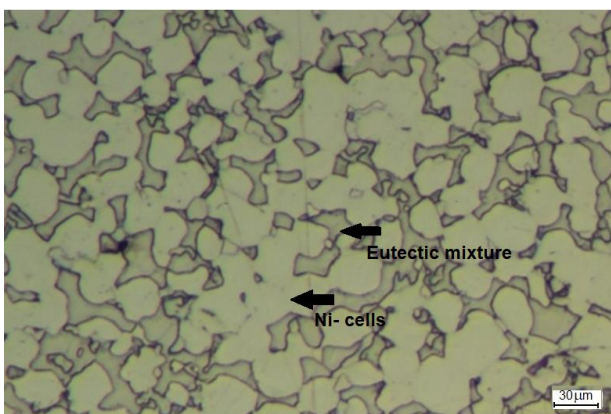


Fig. 8. The microstructure of coating B.

The transition zone between the coating and the substrate shown in Figs. 5, 6 and SEM images showing a detailed view of interface (Figs. 9 and 10) confirmed good adhesion between coating and substrate. These observations correspond to [27], where it is reported that the two-stage deposition process offers good adhesion to the substrate as well as a significant reduction in porosity after the remelting process.

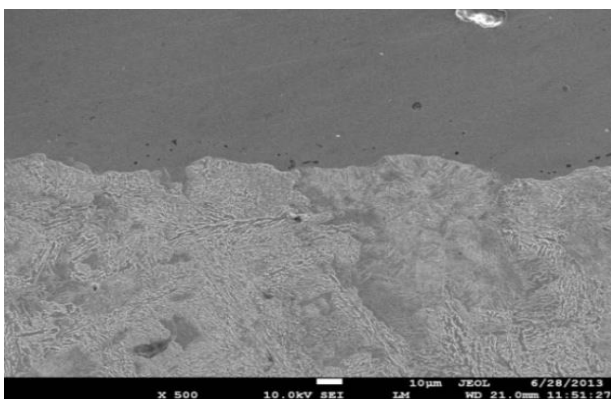


Fig. 9. The coating A/substrate interface.

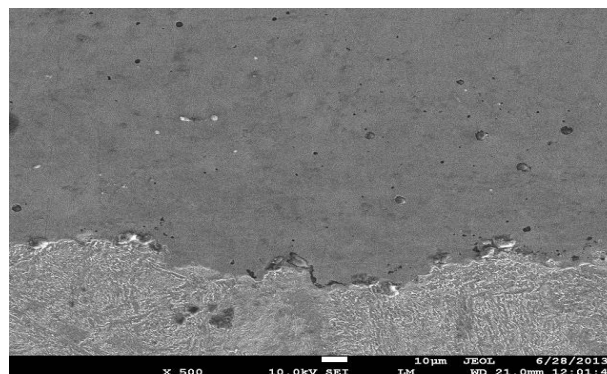


Fig. 10. The coating B/substrate interface.

Heat treatment after the spraying process provides a dense coating with high cohesiveness, reduced porosity, and a strong diffusion bond to low carbon steel substrates, as also reported in [26].

The measured micro-hardness values of coating A ranged from 285 ± 35 to 295 ± 37 HV0.3, and the micro-hardness values of coating B ranged from 385 ± 39 to 429 ± 47 HV0.3. The higher micro-hardness values of coating B are due to the carbide particles present in the coating. The possible reason for the increase of micro-hardness could be the precipitation hardening effect of the nickel alloys [31]. The wear performance of thermally sprayed materials can be difficult to estimate by adopting the principles of wear behavior for traditional engineering materials. Based on experiments, it was observed that increasing the hardness of the materials resulted in a reduction in wear (Table 2). The specific wear rate of coating B was lower compared to coating A. This can be explained by the chromium carbide precipitates in the metal matrix.

Table 2. Hardness and wear rate of coatings A and B.

Coating	Hardness (Rockwell)	Mass loss Δm [g]	Wear rate W_s [mm^3/Nm]. 10^{-7}
A	20.7 ± 2	0.0672	$2.63 \pm 0,13$
B	39.4 ± 2	0.0389	$1.52 \pm 0,6$

SEM analysis of the worn surfaces was carried out (Figs. 11-14). Three-body abrasion is the combination of the micro-cutting wear mechanism and the plastic wear mechanism. The tested coatings show damage caused by cutting and ploughing material removal mechanisms. In coating A, both ploughing and cutting mechanisms acted (Figs. 11 and 12), while in coating B, mainly a cutting mechanism was observed (Figs. 13 and 14). The worn surface of coating B revealed the shallower grooves depth

compared to coating A (Figs. 13 and 14), which is attributed to its higher hardness, resulting in a lower abrasive wear rate.

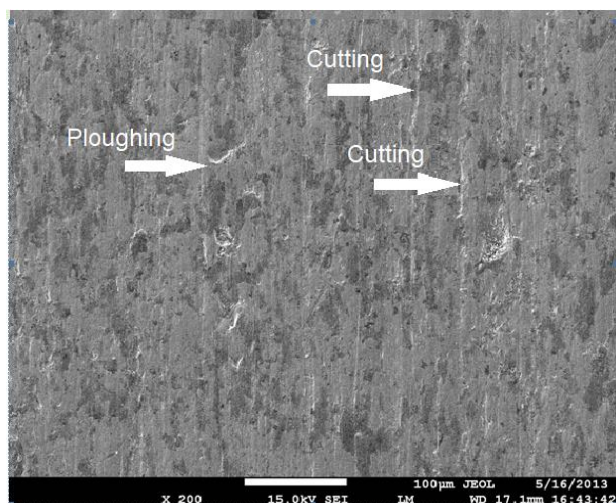


Fig. 11. The worn surface of coating A.

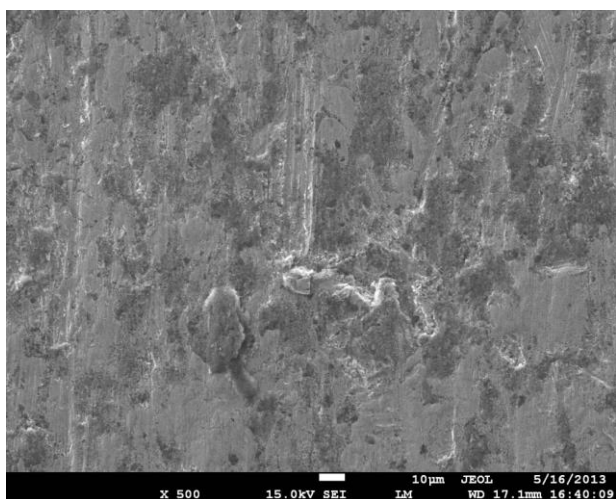


Fig. 12. The worn surface of coating A.

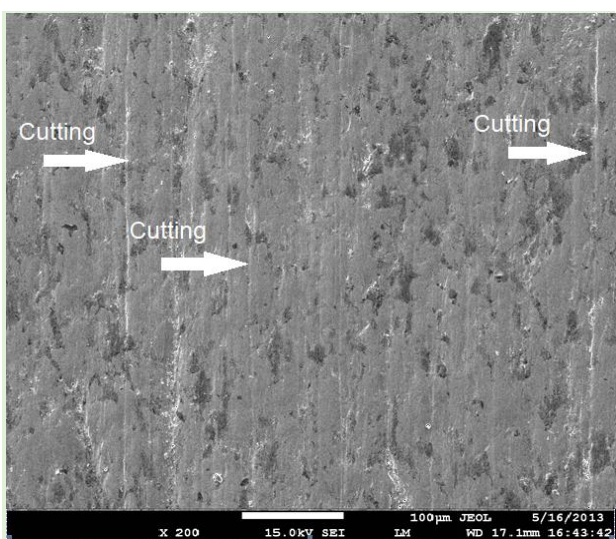


Fig. 13. The worn surface of coating B.

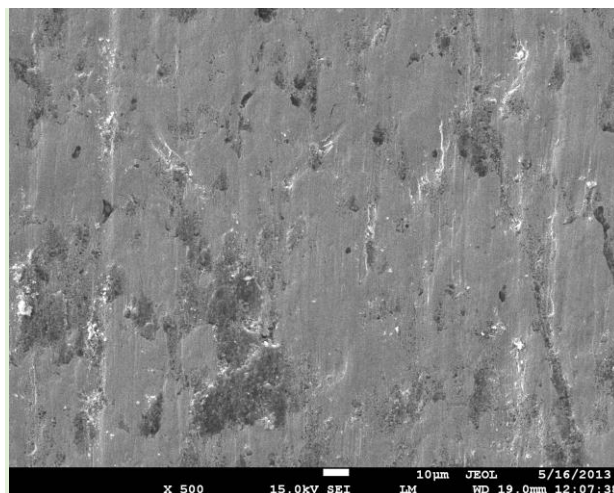


Fig. 14. The worn surface of coating B.

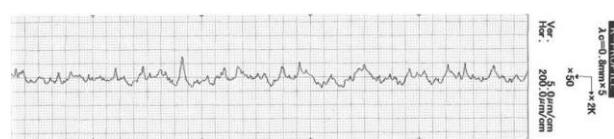


Fig. 15. The surface roughness of coating A after tribotest.



Fig. 16. The surface roughness of coating B after tribotest.

Surface roughness parameters were measured after abrasion tests. Roughness on worn coating surfaces was recorded as follows: coating A: $R_a = 0.65 \mu\text{m}$, $R_z = 5.25 \mu\text{m}$; coating B: $R_a = 0.61 \mu\text{m}$, $R_z = 3.93 \mu\text{m}$. The surface roughness parameters after the abrasion tests show that the deeper grooves observed on the surface of coating A (Figs. 15 and 16) correspond with its higher roughness and lower hardness values compared to coating B.

4. CONCLUSION

The innovative metallic powders with original chemical compositions were deposited by two-step deposition technology and subjected to evaluation of the abrasive wear resistance under three-body wear conditions. Based on the experimental results obtained, the following conclusions can be made:

- The abrasive wear resistance determined by the dry sand rubber wheel test showed an

increased wear resistance of the coating made of powder B compared to coating A.

- The wear resistance and also hardness of coatings A and B correlate with the chemical composition of tested innovative powders.
- The increase of the surface roughness measured by surfmeter and grooves depth of coatings observed by SEM after abrasive test correlates with increased wear rate.
- After the abrasion test, the wear mechanisms of cutting and ploughing were observed on worn surfaces of coatings.
- Tribological characterization of coatings provided information about the efficiency of the chemical composition of the innovative powders determined for the thermal spraying technology.

The thermal spraying, with the various processing techniques and the emerging generation of new materials, remains still in the center of the attention of researchers and industry.

Acknowledgement

This research was funded by the Grant Agency of the Ministry of Education, Science, Research, and Sport of the Slovak Republic under grant VEGA1/0259/19, No.1/0117/15, COST 532, VEGA2/0080/192019-2022, NFP313010T594.

REFERENCES

- [1] R. Rachidi, B. El Kihel, F. Delaunoy, *Microstructure and mechanical characterization of NiCrBSi alloy and NiCrBSi-WC composite coatings produced by flame spraying*, Materials Science and Engineering: B, vol. 241, pp. 13–21, 2019, doi: 10.1016/j.mseb.2019.02.002
- [2] O. Redjail, B. Zaid, M.S. Tabti, K. Henda, P.C. Lacaze, *Characterization of thermal flame sprayed coatings prepared from FeCr mechanically milled powder*, Journal of Materials Processing Technology, vol. 213, iss. 5, pp. 779–790, 2013, doi: 10.1016/j.jmatprotec.2012.11.018
- [3] F. Franek, E. Badisch, M. Kirchgaßner, *Advanced Methods for characterization of abrasion/erosion resistance of wear protection materials*, in 11th International Conference on Tribology - Serbiatrib '09, 13-15 May 2009, Belgrade, Serbia, pp. 27-36.
- [4] Q. Ming, L.C. Lim, Z.D. Chen, *Laser cladding of nickel-based hardfacing alloys*, Surface & Coatings Technology, vol. 106, iss. 2-3, pp. 174–182, 1998, doi: 10.1016/S0257-8972(98)00524-6
- [5] J.M. Miguel, J.M. Guilemany, S. Vizcaino, *Tribological study of NiCrBSi coating obtained by different processes*, Tribology International, vol. 36, iss. 3, pp. 181–187, 2003, doi: 10.1016/S0301-679X(02)00144-5
- [6] T. Hejwowski, S. Szewczyk, A. Weroński, *An investigation of the abrasive and erosive wear of flame-sprayed coatings*, Journal of Materials Processing Technology, vol. 106, iss. 1-3, pp. 54–57, 2000, doi: 10.1016/S0924-0136(00)00638-5
- [7] A. Qu, M. Gouldstone, *On the Role of Bubbles in Metallic Splat Nanopores and Adhesion*, Journal of Thermal Spray Technology, vol. 17, iss. 4, pp. 486–494, 2008, doi: 10.1007/s11666-008-9198-9
- [8] Š. Houdková, E. Smazalová, M. Vostřák, J. Schubert, *Properties of NiCrBSi coating, as sprayed and remelted by different technologies*, Surface and Coatings Technology, vol. 253 pp. 14–26, 2014, doi: 10.1016/j.surfcoat.2014.05.009
- [9] X. Guozhi, Z.J. ingxian, L. Yijun, W. Keyu, M. Xiangyin, L. Pinghua, *Effect of laser remelting on corrosion behavior of plasma-sprayed Ni-coated WC coatings*, Materials Science and Engineering A, vol. 460–461, pp. 351–356, 2007, doi: 10.1016/j.msea.2007.01.064
- [10] S. Harsha, D.K. Dwivedi, A. Agrawal, *Influence of WC addition in Co-Cr-W-Ni-C flame sprayed coatings on microstructure, microhardness and wear behavior*, Surface and Coatings Technology, vol. 201, iss. 12, pp. 5766–5775, 2007, doi: 10.1016/j.surfcoat.2006.10.026
- [11] R. Chotěborský, P. Hrabě, M. Müller, R. Válek, J. Savková, M. Jirka, *Effect of carbide size in hardfacing on abrasive wear*, Research in Agricultural Engineering, vol. 55, pp. 149–158, 2009, doi: 10.17221/1/2009-RAE
- [12] J. Rodríguez, A. Martín, R. Fernández, J.E. Fernández, *An experimental study of the wear performance of NiCrBSi thermal spray coatings*, Wear, vol. 255, iss. 7-12, pp. 950–955, 2003, doi: 10.1016/S0043-1648(03)00162-5
- [13] S. Suman, K. Singh, H.K. Arya, *Improvement in Abrasive Wear Resistance by OxyAcetylene Flame Spraying Method*, International Journal for Research in Applied Science & Engineering Technology (IJRASET), vol. 5, iss. 8, p. 226, 2017, doi: 10.22214/ijraset.2017.8325
- [14] Š. Smetana: *Samotroskotvorný kovový prášok na vytváranie špeciálnych vrstiev-Self-fluxing metal powder for creating special layers*. SK 6336 Y1.

- Úrad priemyselného vlastníctva SK, 2012. (in Slovakian)
- [15] G. Godwin, S.J. Jaisingh, M.S. Priyan, *Tribological and Corrosion Behavior Spray Method- A Review*, Journal of Materials Science & Surface Engineering, vol. 5, iss. 2, pp. 537-543, 2017, doi: [10.1016/j.msse/2348-8956/5-2.4](https://doi.org/10.1016/j.msse/2348-8956/5-2.4)
- [16] A. Maatta, U. Kanerva, P. Vuoristo, *Structure and tribological characteristics of HVOF coatings sprayed from powder blends of Cr3C2-25NiCr and NiCrBSi alloy*, Journal of Thermal Spray Technology, vol. 20, iss. 1-2, pp. 366-371, 2011, doi: [10.1007/s11666-010-9579-8](https://doi.org/10.1007/s11666-010-9579-8)
- [17] X. Wang, M. Zhang, Z. Zou, S. Qu, *Microstructure and properties of laser clad TiC+NiCrBSi+rare earth composite coatings*, Surface and Coatings Technology, vol. 161, iss. 2-3, pp. 195-199, 2002, doi: [10.1016/S0257-8972\(02\)00496-6](https://doi.org/10.1016/S0257-8972(02)00496-6)
- [18] L.F.S. Vieira, H.J.C. Voorwald, M.O.H. Cioffi, *Fatigue Performance Of AISI 4340 Steel Ni-Cr-B-Si-Fe HVOF Thermal Spray Coated*, Procedia Engineering, vol. 114, pp. 606-612, 2015, doi: [10.1016/j.proeng.2015.08.111](https://doi.org/10.1016/j.proeng.2015.08.111)
- [19] I. Hemmati, V. Ocelik, J.Th.M. De Hosson, *Effects of the alloy composition on phase constitution and properties of laser deposition Ni-Cr-B-Si coatings*, Physics Procedia, vol. 41, pp. 302-311, 2013, doi: [10.1016/j.phpro.2013.03.082](https://doi.org/10.1016/j.phpro.2013.03.082)
- [20] M. Fukumoto, H. Wada, K. Tanabe, M. Yamada, E. Yamaguchi, A. Niwa, M. Sugimoto, M. Izawa, *Effect of substrate temperature on deposition behaviour of copper particles on substrate surfaces in the cold spray process*, Journal of Thermal Spray Technology, vol. 16, iss. 5-6, pp. 643-650, 2007, doi: [10.1007/s11666-007-9121-9](https://doi.org/10.1007/s11666-007-9121-9)
- [21] C. Navas, R. Colaço, J. de Damborenea, R. Vilar, *Abrasive wear behaviour of laser clad and flame sprayed-melted NiCrBSi coatings*, Surface and Coatings Technology, vol. 200, iss. 24, pp. 6854-6862, 2006, doi: [10.1016/j.surfcoat.2005.10.032](https://doi.org/10.1016/j.surfcoat.2005.10.032)
- [22] Y. Danlos, S. Costil, X. Guo, H. Liao, C. Coddet, *Ablation laser and heating laser combined to cold spraying*, Surface and Coatings Technology, vol. 205, iss. 4, pp. 1055-1059, 2010, doi: [10.1016/j.surfcoat.2010.06.018](https://doi.org/10.1016/j.surfcoat.2010.06.018)
- [23] E. Zdravecká, M. Ondáč, J. Slota, M. Vojs, M. Marton, *Tribometer pre meranie abratívneho opotrebenia - Tribometer for measurement of abrasion wear, SK200-2015 U1*, Banská Bystrica, ÚPV SR, p. 7, 2017. (in Slovakian)
- [24] I. Hutchings, P. Shipway. *Tribology: friction and wear of engineering materials*, Butterworth-Heinemann, Elsevier, 2017.
- [25] P.J. Blau, K.G. Budinski, *Development and use of ASTM standards for wear testing*, Wear, vol. 225-229, pp. 1159-1170, 1999, doi: [10.1016/S0043-1648\(99\)00045-9](https://doi.org/10.1016/S0043-1648(99)00045-9)
- [26] Z. Bergant, U. Trdan, J. Grum, *Effect of high-temperature furnace treatment on the microstructure and corrosion behavior of NiCrBSi flame-sprayed coatings*, Corrosion Science, vol. 88, pp. 372-386, 2014, doi: [10.1016/j.corsci.2014.07.057](https://doi.org/10.1016/j.corsci.2014.07.057)
- [27] P.C. Vălean, N. Kazamer, D.T. Pascal, R. Muntean, I. Barányi, G. Mărginean, V.A. Șerban, *Characteristics of Thermally Sprayed NiCrBSi Coatings before and after Electromagnetic Induction Remelting Process*, Acta Polytechnica Hungarica, vol. 16, no. 3, pp. 7-18, 2019, doi: [10.12700/APH.16.3.2019.3.1](https://doi.org/10.12700/APH.16.3.2019.3.1)
- [28] H. Okamoto, M.E. Schlesinger, E.M. Mueller. *ASM Handbook Volume 3: Alloy Phase Diagrams*. ASM International, 2016.
- [29] H.-J. Kim, S.-Y. Hwang, C.-H. Lee, P. Juvanon, *Assessment of wear performance of flame sprayed and fused Ni-based coatings*, Surface and Coatings Technology, vol. 172, iss. 2-3, 2003, doi: [10.1016/S0257-8972\(03\)00348-7](https://doi.org/10.1016/S0257-8972(03)00348-7)
- [30] R. Rachidi, B. El Kihel, F. Delaunois, V. Vitry, D. Deschuyteneer, *Wear Performance of Thermally Sprayed NiCrBSi and NiCrBSi-WC Coatings Under Two Different Wear Modes*, Journal of Materials and Environmental Sciences, vol. 8, iss. 12, pp. 4550-455, 2017.
- [31] E. Fernández, M. Cadenas, R. González, C. Navas, R. Fernández, J. de Damborenea, *Wear behaviour of laser clad NiCrBSi coating*, Wear, vol. 259, iss. 7-12, pp. 870-875, 2005, doi: [10.1016/j.wear.2005.02.063](https://doi.org/10.1016/j.wear.2005.02.063)